Final Scientific Report

DE-FG02-05ER15660

University of California, Riverside

Fundamental Studies of Energy- and Hole/Electron-Transfer in Hydroporphyrin Architectures

David F. Bocian

Executive Summary

The long-term objective of the research program is to design, synthesize, and characterize tetrapyrrole-based molecular architectures that absorb sunlight, funnel energy, and separate charge with high efficiency and in a manner compatible with current and future solar-energy conversion schemes. This effort is highly collaborative. The J. S. Lindsey group (N. C. State University) focuses on design, synthesis, and chemical characterization of synthetic molecular architectures, which are then subjected to physicochemical and photophysical characterization by the Bocian (UC, Riverside), and D. Holten & C. Kirmaier groups (Washington University). Collectively, the studies have lead to a better understanding of organic molecular architectures can be implemented for solar-energy conversion. Solar-energy conversion based on such molecular architectures can potentially reduce reliance on non-renewable energy sources such as petrochemical materials.

Goals and Accomplishments of the Project

All of the goals of the project have been met. These accomplishments are as follows: (1) The rates of ground-state hole transfer in covalently linked tetrapyrrolic dyads and larger arrays have been measured to probe the effects of molecular characteristics (macrocycle and linker) on the dynamics. (2) The structural, spectral, electronic, and photophysical properties of a large number of synthetic chlorins and bacteriochlorins have been probed with the aim of controlling spectral coverage and excited-state lifetimes. (3) Tthe spectral and photophysical properties of a series of novel perylene–tetrapyrrole dyads have been examined. (4) Additional synthetic methods have been developed that allow broad-based access to chlorins and bacteriochlorins that bear unique substituents. This research has led to 20 publications. Most are full papers with complete descriptions of synthetic methods and detailed physicochemical studies; most are in journals of scholarly societies (ACS, RSC, or ASP).

Project Activities
The Table of Contents below lists how the research performed is presented in this final report.

Table of Contents

1. EPR Studies Ground-State Hole/Electron Transfer in Covalently Linked Arrays.

1.1. Dyads - Effects of Linker Torsional Constraints.[11] Understanding hole/electron-transfer processes among interacting constituents of multicomponent molecular architectures is central to the fields of artificial photosynthesis and molecular electronics. We utilized a recently demonstrated $^{203}Tl/^{205}Tl$ hyperfine "clocking" strategy to probe the rate of hole/electron transfer in the monocations of a series of three thallium-chelated porphyrin dyads, designated **Tl_2-U**, **Tl_2-M**, and **Tl_2-B**, that are linked via diarylethynes wherein the number of *ortho*-dimethyl substituents on the aryl group of the linker systematically increases (none, one, and two, respectively; Chart 1).

Variable-temperature (160–340 K) EPR studies on the monocations of the three dyads were used to examine the thermal activation behavior of the hole/electron-transfer process (Figure 1). The activation behavior was modeled using the semiclassical Marcus equation in the nonadiabatic limit (Eq. 1),

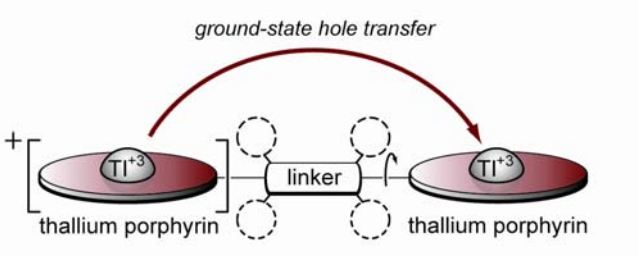

Chart 1. Torsionally constrained dyads.

$$k = AT^{-1/2}\exp(-\Delta G^{\ddagger}/k_BT) \qquad (1)$$

where $\Delta G^{\ddagger} = (\Delta G_o + \lambda)^2/4\lambda$; $A = (4\pi^3/h^2\lambda k_B)^{1/2} |V^2|$; ΔG_o is the free energy change associated with hole/electron transfer; λ is the reorganization energy; and V is the effective electronic coupling. The Marcus-equation plots for the three dyads are shown in Figure 2 and reveal the following: (1) Hole/electron transfer at room temperature (295 K) slows as torsional constraints are added to the diarylethyne linker [k(**Tl_2-U**) > k(**Tl_2-M**) > k(**Tl_2-B**)], with rate constants that

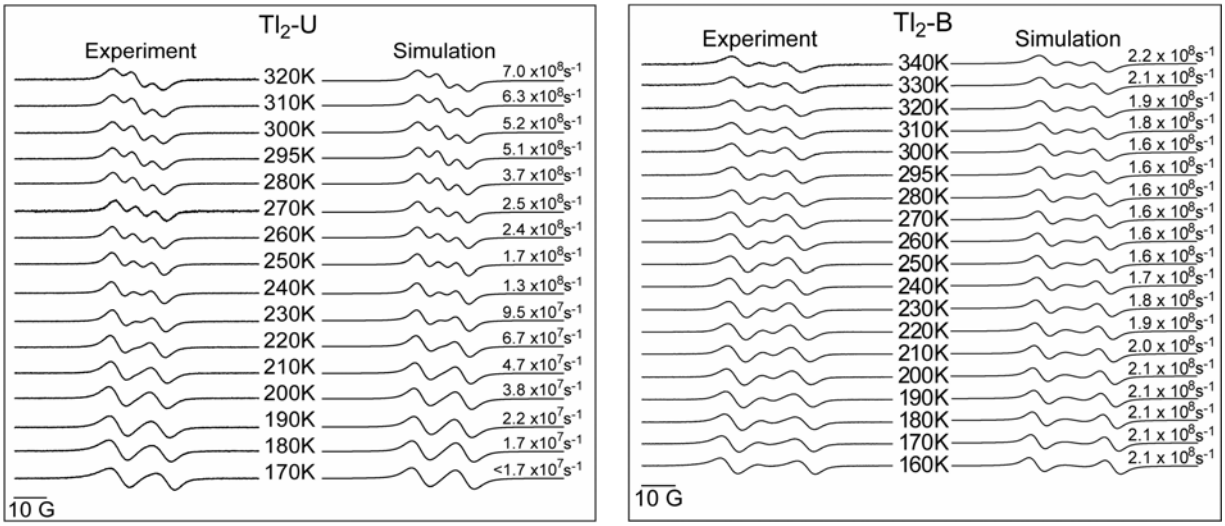

Figure 1. Variable-temperature EPR spectra the unhindered dyad **Tl_2-U** (left panel) and bishindered dyad **Tl_2-B**. (right panel). The left traces in each panel are the exerimental spectra and the right traces are simulations and derived hole/electron-transfer rates.

correspond to time constants in the 2–5 nanosecond regime. (2) As the temperature decreases, the hole/electron-transfer rates for the monocations of the three types of dyads converge and then cross over. At the lowest temperatures examined (160–170 K), the trend in the hole/electron-transfer rates is essentially reversed [k (**Tl_2-B**) > k(**Tl_2-M**) ~ k(**Tl_2-U**)]. The trends in the temperature dependence of hole/electron-transfer among the three dyads are consistent with torsional motions of the aryl rings of the linker providing for thermal activation of the process at higher temperatures in the case of the less torsionally constrained dyads, **Tl_2-U** and **Tl_2-M**. In the case of the most torsionally constrained dyad, **Tl_2-B**, the hole/electron-transfer process is activationless at all temperatures studied. The reversal in rates of hole/electron transfer among the three dyads at low temperature is qualitatively explained by the results of DFTcalculations, which predict that static electronic factors could dominate the hole/electron-transfer process when torsional dynamics are thermally diminished.

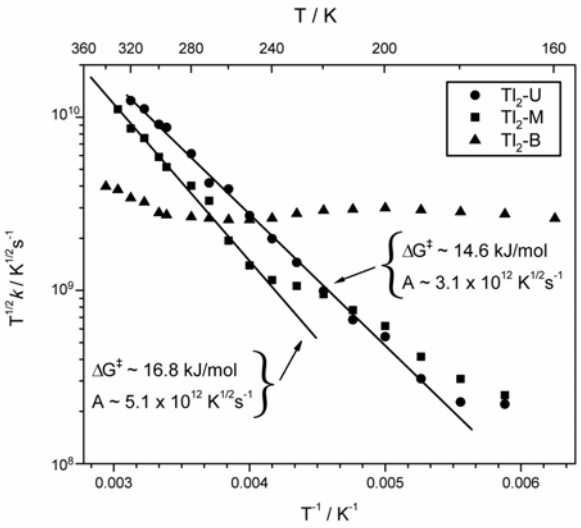

Figure 2. Marcus-equation plots for the monocations of **Tl_2-U**, **Tl_2-M**, and **Tl_2-B**.

1.2. Larger Arrays. The EPR studies of the thallium-chelated arrays have been extended to a series of triadic systems (Chart 2). Each array is terminated by a thallium-chelated trimesityl-porphyrin; the linkers are diphenylethyne. The triads differ only in the nature of the non-linking substituents on the central porphyrin: **Tl-Fb-Tl**, free-base dimesitylporphyrin; **Tl-Tl-Tl**, thallium-chelated dimesitylporphyrin; **Tl-Fb(F_{10})-Tl**, free base di(pentafluoro)porphyrin; **Tl-Tl(F_{10})-Tl**, thallium-chelated di(pentafluorophenyl)pophyrin. The EPR studies indicate the

following: (1) For **Tl-Fb-Tl**, the hole is localized on the central porphyrin. (2) for both **Tl-Fb(F_{10})-Tl** and **Tl-Tl(F_{10})-Tl**, the hole transfer is slow on the EPR timesacale ($<10^5$ s^{-1}). (3) Only in the case of **Tl-Tl-Tl** is the hole/electron-tranfser rate ($\sim10^8$ s^{-1}) measurable via the EPR clocking method. These results can be explained by the relative redox potentials of the terminal versus central porphyrins. This time scale for hole transfer in **Tl-Tl-Tl** is similar to that of a dyad with the same linker. Variable temperature EPR studies of the triad indicate that the activation barrier for hole transfer is somewhat larger than for the dyad (20 vs 15 kJ/mol).

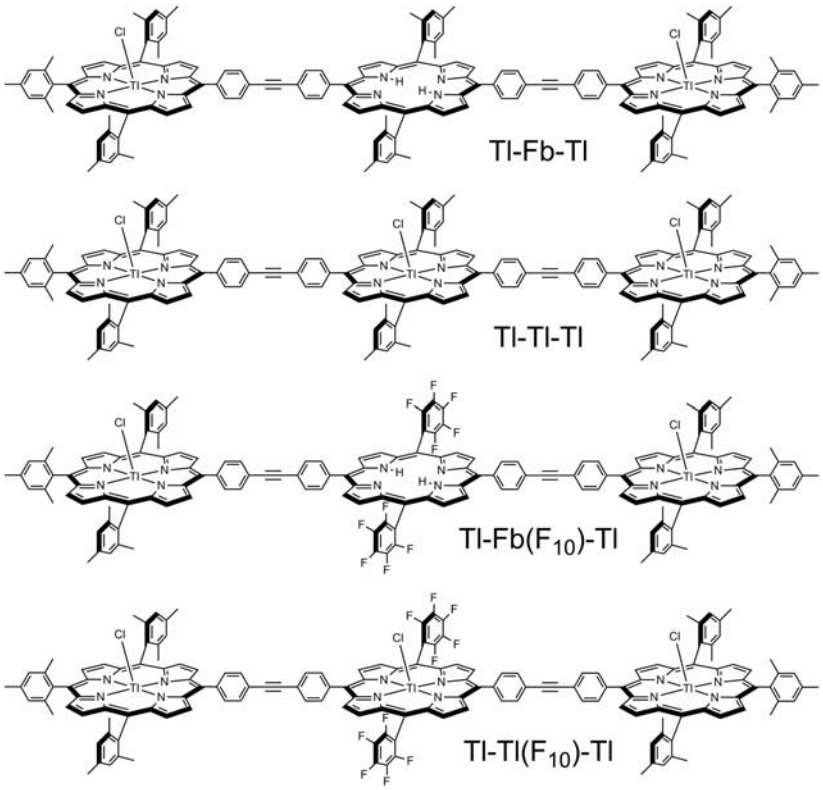

Chart 2. Triads for hole-transfer studies.

2. Structural, Electronic and Photophysical Properties of Synthetic Chlorins.

2.1. Sparsely-Substituted Chlorins.[1] Understanding the effects of substituents on natural photosynthetic pigments should provide for a more thoughtful design of artificial light-harvesting systems. The hydrocarbon skeleton of all chlorophylls is phorbine, which contains an annulated five-membered (isocyclic) ring in addition to the reduced pyrrole ring characteristic of chlorins (Chart 3). To probe how these structural features affect the spectral and photophysical properties of the molecule, a phorbine and a 13^1-oxophorbine (which bears an oxo group in the isocyclic ring) were synthesized (Chart 3). The phorbine and 13^1-oxophorbine macrocycles lack peripheral substituents other than a geminal dimethyl group in the reduced ring to stabilize the chlorin chromophore. The spectral properties and electronic structure of the zinc or free base 13^1-oxophorbine closely resemble those of the corresponding analogues of chlorophyll *a*. Accordingly, the fundamental electronic properties of chlorophylls are primarily a consequence of the 13^1-oxophorbine base macrocycle.

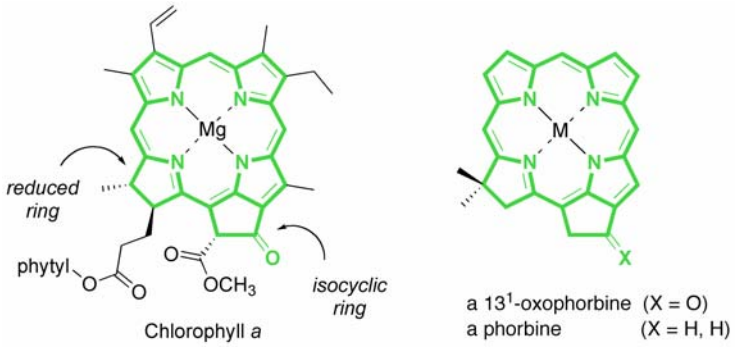

Chart 3. Structure of chlorophyll *a* and sparsely substituted synthetic analogues.

2.2. Axochrome-Substituted Chlorins. ***2.2.1. The effects of substituents at the 7- versus 3,13-positions.***[8] Chlorophyll *a* and *b* differ solely in the nature of the 7-substituent (methyl versus formyl) whereas chlorophyll *a* and *d* differ solely in the 3-substituent (vinyl versus formyl), yet have distinct long-wavelength absorption maxima: 665 nm (*a)* 646 nm (*b*), and 691 nm (*d*). We explored the origin of these spectral differences as a logical step toward the design of chlorin-based light-harvesting systems. To this end, we examined the spectra, singlet excited-state decay properties, and molecular-orbital characteristics (from DFT calculations) of synthetic chlorins and 13[1]-oxophorbines that contain ethynyl, acetyl, formyl and other groups at the 3-, 7- and/or 13-positions (Chart 4).

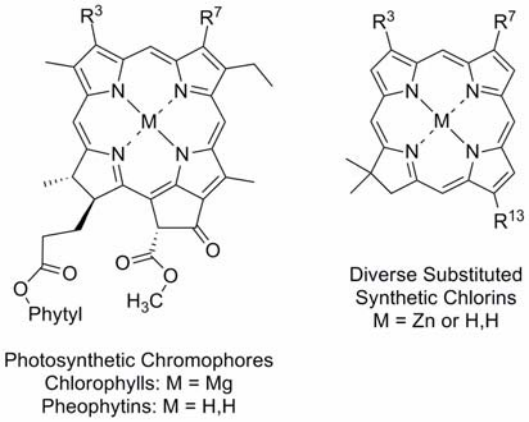

Chart 4. Natural chlorophylls and auxochrome-substituted synthetic analogues.

We found that the substituent effects on the absorption spectra are well accounted for using Gouterman's four-orbital model. The key findings are that (1) the dramatic difference in auxochromic effects of a given substituent at the 7- versus 3- or 13-positions primarily derives from relative effects on the LUMO+1 and LUMO; (2) formyl at the 7- or 8-position effectively "porphyrinizes" the chlorin; and (3) the substituent effect increases in order of vinyl < ethynyl < acetyl < formyl. Thus, the spectral properties are governed by an intricate interplay of electronic effects of substituents at particular sites on the four frontier molecular orbitals of the chlorin macrocycle.

2.2.2. Chlorins bearing one to four meso-substitutents.[17] We examined the effects of meso-substituents on the basic chlorin macrocycle. These studies were enabled via the development of new synthetic methods. Prior syntheses provided access to chlorins bearing distinct aryl substituents (individually or collectively) at the 5, 10, and 15-positions, but not the 20-position. A new Western half (5-phenyl-2,3,4,5-tetrahydro-1,3,3-trimethyldipyrrin) was employed in condensation with an Eastern half (9-bromodipyrromethane-1-carboxaldehyde) followed by oxidative cyclization to give (5% yield) the zinc(II) 20-phenylchlorin. Condensation of the same Western half and a diaryl-substituted Eastern half provided (11% yield) the zinc(II) 5,10,20-triarylchlorin; demetalation with TFA followed by 15-bromination and Suzuki coupling gave the free base 5,10,15,20-tetraarylchlorin. Altogether, 10 new synthetic chlorins were prepared and studied. The long-wavelength (Q_y) absorption band undergoes a bathochromic and hypochromic shift in concert with a bathochromic shift of the near-UV features with increasing number of meso-aryl groups (Figure 3).

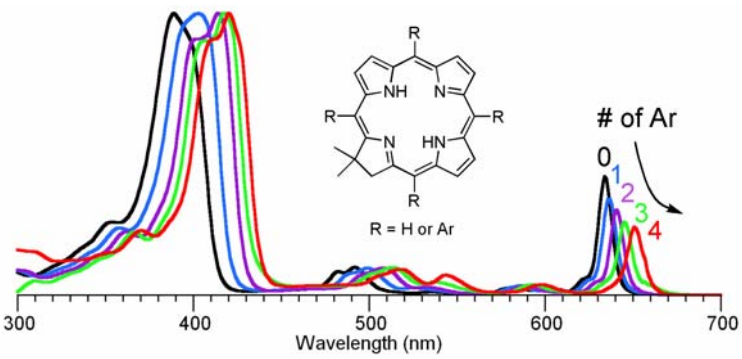

Figure 3. Absorption spectra of chlorins with meso-aryl substituents.

Regardless of the number and positions of the meso-aryl groups (including "walking a phenyl group around the ring"), the fluorescence quantum yields (0.17–0.27) and singlet excited-

state lifetimes (9.4–13.1 ns) are comparable among the free base chlorins and similarly for the zinc chelates (0.057–0.080; 1.2–1.6 ns). DFT calculations show that of the chlorin frontier molecular orbitals, the energy of the HOMO-1 is the most affected by meso-aryl substituents, undergoing progressive destabilization as the number of meso-aryl groups is increased. The availability of chlorins with 0–4 distinct meso-aryl substituents provides the individual stepping-stones to bridge the known unsubstituted chlorin and the *meso*-tetraarylchlorins.

2.2.3. Chlorin-chalcones.[18] The ability to tailor synthetic chlorins with diverse substituents about the macrocycle perimeter – and thereby tune spectral and photophysical features – prompted us to examine conjugated substituents known as chalcones (i.e., enones). A chalcone of great interest was obtained by reaction of all-*trans*-retinal with the 13-acetylchlorin (Chart 5). The spectral and photophysical properties (Φ_f, τ_s, k_f, k_{ic}, k_{isc}) of four chlorin–chalcones (retinylidene or benzylidene; zinc or free base) along with benchmarks (no group or acetyl at the 13-position) were examined. These studies were accompanied by DFT calculations that probe the characteristics of the frontier molecular orbitals. The chlorin–chalcones in nonpolar (toluene) and polar (dimethylsulfoxide) media exhibit bathochromically shifted (and intense) Q_y absorption bands. The presence of the retinylidene group adds new absorption in the 450–500 nm region where the chlorins are typically transparent; excitation in this region leads to quantitative formation of the chlorin Q_y excited state. Representative absorption spectra are shown in Figure 4. The four chlorin–chalcones in the solvent toluene have high fluorescence yields (0.24–0.30) and long singlet excited-state lifetimes (3.7–8.4 ns). The results provide further fundamental insight into tuning the properties of chlorins, including providing absorption in the normally transparent region between the Soret and Q_x bands.

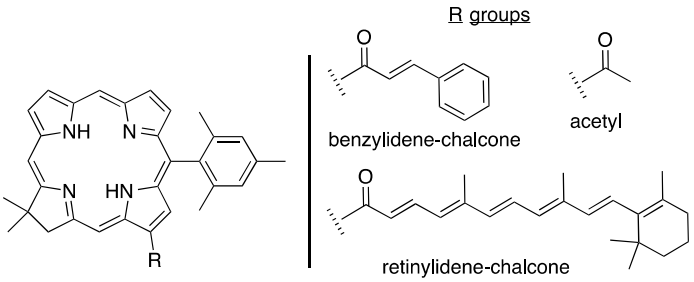

Chart 5. Chlorin-chalcones.

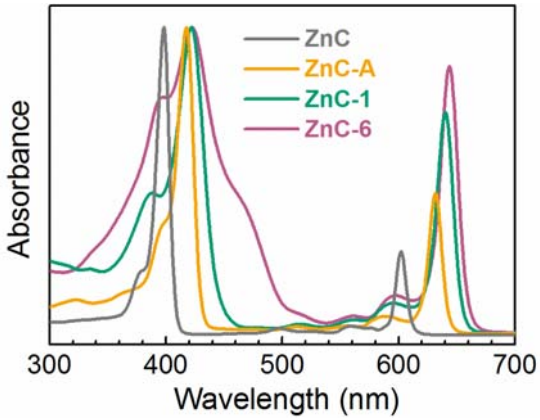

Figure 4. Normalized absorption spectra of the zinc chlorins in toluene.

3. Structural, Electronic and Photophysical Properties Synthetic Bacteriochlorins.

3.1. Auxochrome-Substituted Free Base Bacteriochlorins. ***3.1.1. A palette of NIR absorbing tetrapyrroles.***[6] Bacteriochlorins, which are tetrapyrrole macrocycles with two reduced pyrrole rings, are Nature's near-infrared (NIR) absorbers (700–900 nm). The strong absorption in the NIR region renders bacteriochlorins excellent candidates for solar light harvesting. Regardless, natural bacteriochlorins are inherently unstable due to oxidative conversion to the chlorin (one reduced pyrrole ring) or the porphyrin. The natural pigments are also only modestly amenable to synthetic manipulation, owing to a near full complement of substituents on the macrocycle. Recently, new synthetic methodology has afforded access to stable synthetic

bacteriochlorins wherein a wide variety of substituents can be appended to the macrocycle at preselected locations.

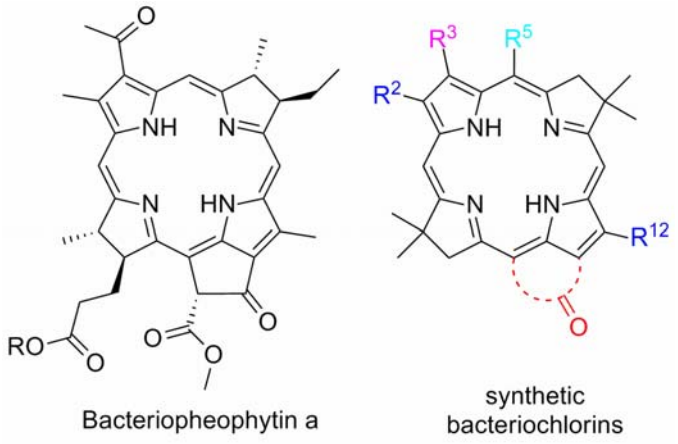

Figure 5. Absorption spectra of representative synthetic bacteriochlorins.

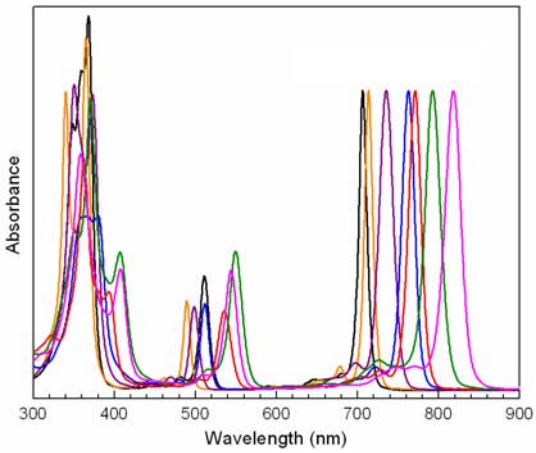

Chart 6. Bacteriopheophytin *a* and auxochromic synthetic analogues.

This methology was used to prepare a large number of synthetic free base (metal free) bacteriochlorins; the spectroscopic and photophysical properties of 33 such bacteriochlorins were investigated. These synthetic chromophores contained substituents at the 2, 3, 5, and 12 positions of the macrocycle (Chart 6). The NIR absorption bands of the chromophores range from ~700 to ~820 nm (Figure 5); the lifetimes of the lowest excited singlet state range from ~2 to ~6 ns; the fluorescence quantum yields range from ~0.05 to ~0.25; the average yield of the lowest triplet excited state is ~0.5. DFT calculations indicate that the impact of substituents on the spectral properties of the molecules derives primarily from effects on the LUMO. The studies show how the palettes of synthetic bacteriochlorins extend the properties of the native photosynthetic pigments (bacteriochlorophylls) and provide a fundamental electronic basis for understanding these properties.

3.1.2. Bacteriochlorin-chalcones.[14] The studies were extended to include the synthesis and characterization of nine free base bacteriochlorins containing the more highly conjugated chalcone (i.e., enone) substituents, including one related to all-*trans*-retinal (Chart 7). Again, the photophysical properties (τ_s, Φ_f, Φ_{ic}, Φ_{isc}, τ_T, k_f, k_{ic}, k_{isc}) and molecular orbital characteristics were examined. The bacteriochlorin-chalcones absorb strongly in the 780–800 nm region and have fluorescence yields in the range 0.05–0.11 in toluene and dimethylsulfoxide. Light-induced electron promotions between orbitals with primarily substituent or macrocycle character or both may give rise to some net macrocycle ↔ substituent charge-transfer character in the lowest and higher singlet excited states as indicated by DFT and time-dependent DFT calculations. Such calculations indicated significant participation of molecular orbitals beyond those (HOMO-1 to LUMO+1) in the Gouterman four-orbital model. The studies further elucidate the design principles for tuning the spectral and photophysical properties of these NIR-absorbing tetrapyrroles.

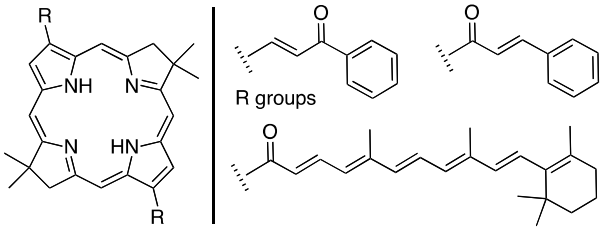

Chart 7. Bacteriochlorin–chalcones.

3.2. Diverse Metallobacteriochlorins.[5,9,10,12,13] Bacteriochlorins have wide potential in photochemistry due to their strong absorption of near-infrared light, yet metallobacteriochlorins traditionally have been accessed with difficulty. Established acid-catalysis conditions [$BF_3{\cdot}OEt_2$ in CH_3CN or TMSOTf/2,6-di-*tert*-butylpyridine in CH_2Cl_2] for the self-condensation of dihydrodipyrrin-acetals (bearing a geminal dimethyl group in the pyrroline ring) afford stable free base bacteriochlorins. We found that $InBr_3$ in CH_3CN at room temperature gives directly the corresponding indium bacteriochlorin (Chart 8).

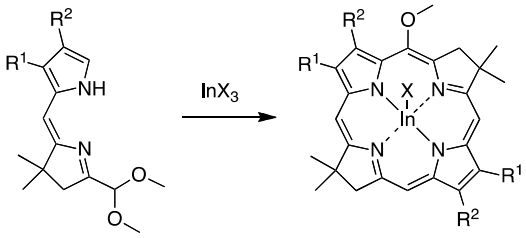

Chart 8. Synthesis of indium bacteriochlorins.

Application of the new acid catalysis conditions has afforded four indium bacteriochlorins bearing aryl, alkyl/ester, or no substituents at the β-pyrrolic positions. Compared to the free base analogues, the indium bacteriochlorins exhibit a bathochromically shifted (by 23–31 nm) absorption band (741–782 nm) along with reduced fluorescence quantum yield (0.011–0.026) and singlet excited-state lifetime (270 ps average). The trends in optical properties of the indium bacteriochlorins versus free base analogues correlate well with frontier molecular-orbital energies and energy gaps derived from DFT calculations. The corresponding differences in the excited-state properties derive primarily from a 30-fold greater rate constant for $S_1 \rightarrow T_1$ intersystem crossing, which stems from the heavy-atom effect on spin-orbit coupling.

Substantial effort was required to develop procedures to prepare bacteriochlorins containing a variety of other metals including Mg, Cu, Zn, and Pd (Chart 9). We examined members of a set of synthetic bacteriochlorins bearing 0–4 carbonyl groups (1, 2, or 4 carboethoxy substituents, or an annulated imide moiety) under two conditions: (i) standard conditions for zincation of porphyrins [$Zn(OAc)_2{\cdot}2H_2O$ in DMF at 60–80 °C], and (ii) treatment in THF with a strong base (e.g., NaH or LDA) followed by a metal reagent MX_n. The details of the specific method necessary were found to depend on metal and the number of electron-withdrawing groups on the macrocycle. Altogether, 15 metallobacteriochlorins were isolated and characterized. Single-crystal X-ray analysis of 8,8,18,18-tetramethylbacteriochlorin revealed that the core geometry provided by the four nitrogen atoms is rectangular; the difference in length of the two sides is ~0.08 Å. Electronic characteristics of (metal-free) bacteriochlorins were probed through electrochemical measurements along with DFT calculation of the energies of the frontier molecular orbitals. The photophysical properties (Φ_f, Φ_T, τ_S, τ_T) of the zinc bacteriochlorins are generally similar to those of the metal-free analogues, and to those of the native chromophores bacteriochlorophyll *a* and bacteriopheophytin *a*.

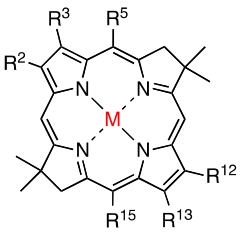

Chart 9. Metallo-bacteriochlorins.

As part of the studies of synthetic bacteriochlorins, we also examined the relationships involving metal ion (e.g., Zn, Pd, free base), macrocyle substituents, solvent (polar and nonpolar organic solvents, aqueous micellar solutions), photophysical properties (singlet and triplet excited states), redox characteristics, presence and absence of oxygen, solubility, and photostability of the bacteriochlorins. Collectively, the results and the availability of diverse metallobacteriochlorins should prove useful in a variety of fundamental photochemical studies and applications.

4. Perylene–Tetrapyrrole Dyads.

4.1 Strongly Coupled Dyads.[15] The synthesis, photophysical, redox, and molecular-orbital properties of three perylene–tetrapyrrole dyads were investigated to elucidate characteristics favorable for use in next-generation light-harvesting assemblies. Each dyad contains a common perylene-monoimide that is linked at the 9-position via an ethynyl group to the meso-position of the tetrapyrrole. The tetrapyrroles include a porphyrin, chlorin, and bacteriochlorin, which have zero, one, and two reduced pyrrole rings, respectively (Chart 10). The increased pyrrole-ring reduction results in a progressive red shift and intensification of the lowest-energy absorption band, as exemplified by benchmark monomers (Figure 6). The direct ethyne linkage and accompanying strong perylene–tetrapyrrole electronic coupling in the dyads is evident by significant differences in optical absorption versus the sum of the features of the constituents. The perturbations decrease for the tetrapyrrole constituent along the series porphyrin > chlorin > bacteriochlorin. This trend is explained by the relative configurational mixing in the tetrapyrrole excited states and how the configuration-interaction energy (and not simply the energies of the configurations) is affected by coupling to the perylene. The perylene–tetrapyrrole electronic coupling is further evidenced in the redox and molecular-orbital characteristics of the three dyads. All three dyads in nonpolar solvents exhibit relatively long singlet excited-state lifetimes (3.3–6.5 ns) and relatively large fluorescence quantum yields (0.14–0.40). Collectively, the physicochemical characteristics of the strongly coupled perylene–tetrapyrrole dyads render these architectures excellent candidates for light-harvesting materials with significant, even panchromatic, near-ultraviolet to near-infrared absorption.

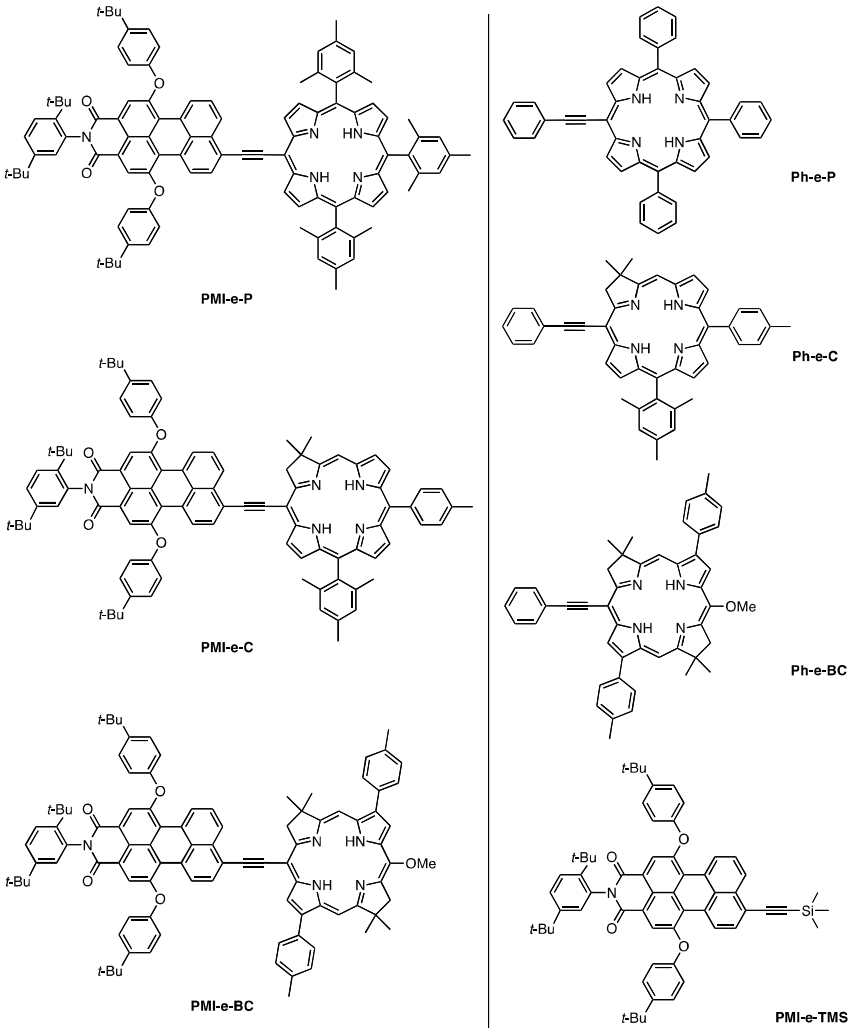

Chart 10. Perylene–tetrapyrrole dyads (left) and benchmarks (right).

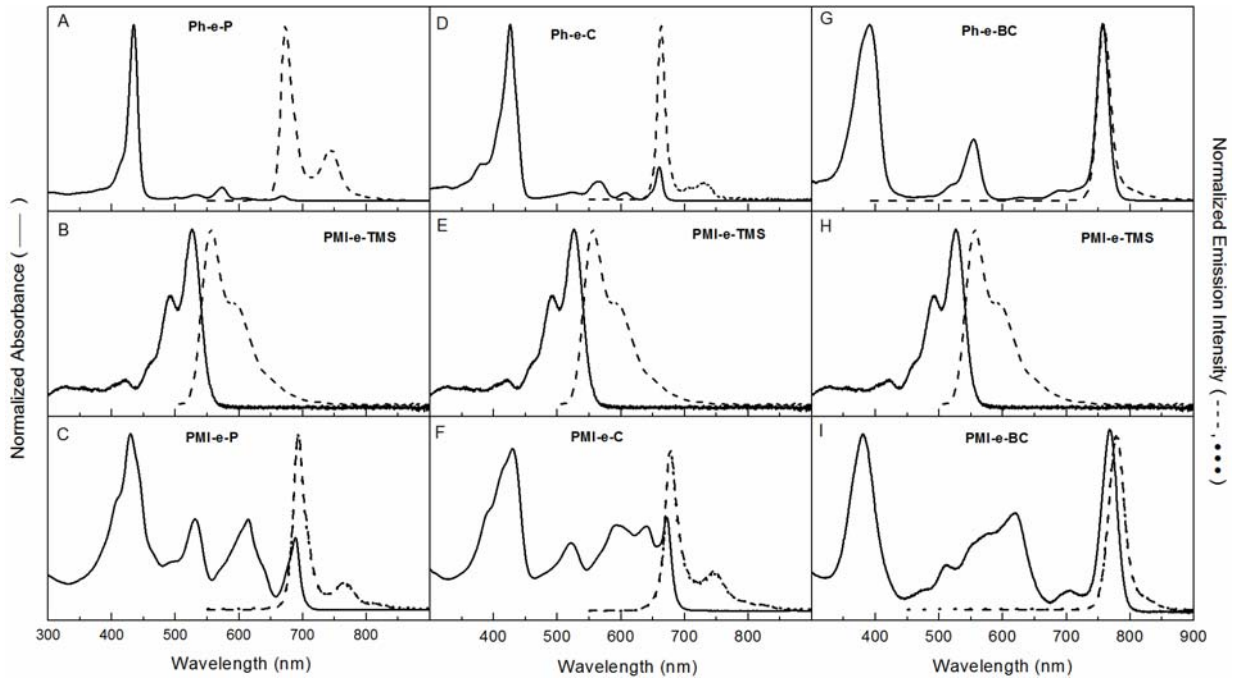

Figure 6. Absorption (solid) and fluorescence spectra of the perylene–tetrapyrrole arrays. Note the panchromatic absorption of the dyads (bottom row). In each column, the dyad absorption is not the sum of the parts (tetrapyrrole + perylene).

4.2 Arylethyne-Linked Dyads.[19] As a complement to the strongly coupled perylene-trapyrroles described above, a trio of perylene-tetrapyrrole dyads with less strong electronic interactions between the constituents was prepared. This second set of dyads again has a common perylene-monomide attached to a porphyrin, chlorin, or bacteriochlorin, but with a different connection motif. In particular, this second set has the aryl group of an arylethyne linker attached to the perylene N-imide position and the ethyne group to the tetrapyrrole meso-position (Chart 11). These dyads exhibit optical spectra that are the sum of the spectra of the constituents and redox potentials virtually identical to those of the benchmark components. These observations and the molecular orbital characteristics (energies and electron density distributions) of the dyads versus the benchmarks indicate relatively weak electronic coupling between the constituents. However, the perylene-tetrapyrrole interactions are sufficiently strong to support ultrafast (0.5–3 ps) and virtually quantitative (>98%) energy transfer from excited perylene to tetrapyrrole in all three dyads. The subsequent decay of the excited tetrapyrrole (as evidenced by fluorescence yield and singlet lifetime) is basically the same as in the isolated tetrapyrrole for all three dyads in toluene and for the porphyrin dyads in dimethylesulfoxide. Relatively small excited-state quenching is observed for the chlorin and bacteriochlorin dyads in dimethylsulfoxide, which can be understood in terms of a low yield of porphyrin-to-perylene electron transfer. Collectively, the studies indicate that the perylene-tetrapyrrole motif utilized in these dyads is quite favorable of light-harvesting complexes that basically preserve (the sum of) the absorption properties of the constituents. Thus, this set of dyads and the strongly coupled counterparts that exhibit panchromatic absorption provide complementary properties for arrays that utilize all three main classes of tetrapyrroles (porphyin, chlorin, bacteriochlorin).

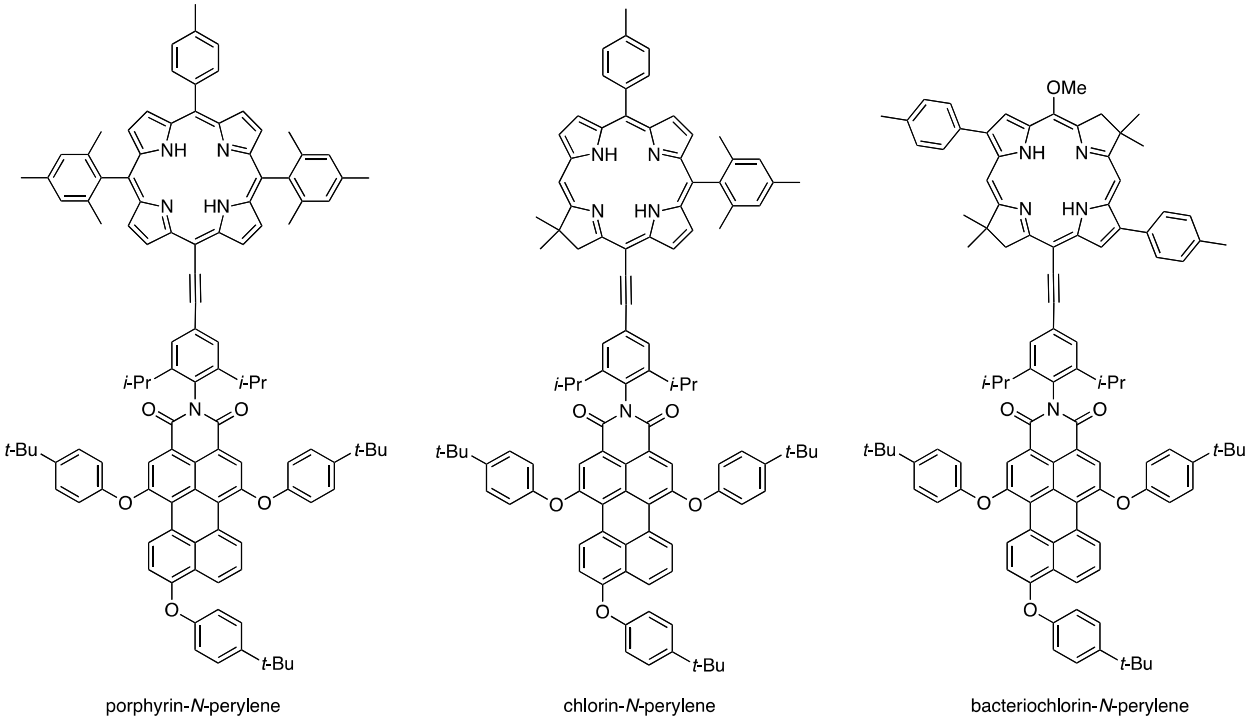

Chart 11. Perylene–tetrapyrrole dyads (moderately coupled) for studies of energy transfer.

5. Synthesis[2,4,5,712,16,17]

The porphyrins and hydroporphyrins displayed above were all prepared in the Lindsey lab upon consultation with collaborators Bocian and Holten&Kirmaier so as to pursue our mutual objectives in energy-sciences research. The advances in synthetic methodology that have provided access to the diverse target molecules will not be reiterated here; suffice it to say that (i) porphyrins bearing 0-4 meso substituents, including four different meso substituents, are now readily accessible; (ii) stable synthetic chlorins are available where a given substituent can be introduced at any of the six β-pyrrole, four meso-, or two β-pyrrolinyl sites, and multiple substitutions can be achieved to create patterned chlorins; (iii) stable synthetic bacteriochlorins are now available that bear a variety of different substituents.

Methods for installing the isocyclic ring (ring E) on chlorins to give the 13^1-oxophorbine or phorbine, the fundamental framework of chlorophylls, also have been developed and exploited. A key advance in the present period was the synthesis of chlorins with 0–4 meso-substituents. The range of chlorins that have become available with advances in synthesis now encompass diverse building blocks for incorporation into arrays, macrocycles bearing one or more isotopic labels at designated sites, and sparsely substituted ("naked") analogues of chlorophylls.

The synthetic methodology for preparing bacteriochlorins is less developed than that of chlorins and porphyrins. One advance in the present granting period was a deeper understanding of metalation chemistry. The ease of metalation of porphyrinic macrocycles decreases in the following order: porphyrin > chlorin > bacteriochlorin. Although we have prepared 140 synthetic bacteriochlorins (including free base and diverse metal chelates), it is perhaps most informative to describe what cannot yet be done with ease in bacteriochlorin chemistry: (a) Install distinct substituents in the two pyrrole rings (A and C); in other words, because the bacteriochlorin macrocycle is created by dimerization of dihydrodipyrrin-acetals, whatever

substituent is present in the pyrrolic unit appears both in rings A and C. (b) Derivatize the four meso positions of the bacteriochlorin in a controlled (ideally sequential) manner.

6. Bibliography of Published Work

(1) "Structural Characteristics that Make Chlorophylls Green: Interplay of Hydrocarbon Skeleton and Substituents," Mass, O.; Taniguchi, M.; Ptaszek, M.; Springer, J. W.; Faries, K. M.; Diers, J. R.; Bocian, D. F.; Holten, D.; Lindsey, J. S. *New J. Chem.* **2011**, *35*, 76–88.

(2) "De Novo Synthesis and Photophysical Characterization of Annulated Bacteriochlorins. Mimicking and Extending the Properties of Bacteriochlorophylls," Krayer, M.; Yang, E.; Diers, J. R.; Bocian, D. F.; Holten, D.; Lindsey, J. S. *New J. Chem.* **2011**, *35*, 587–601.

(3) "Tapping the Near-Infrared Spectral Region with Bacteriochlorin Arrays," Lindsey, J. S.; Mass, O.; Chen, C.-Y. *New J. Chem.* **2011**, *35*, 511–516.

(4) "Facile Synthesis of a B,D-Tetradehydrocorrin and Rearrangement to Bacteriochlorins," Aravindu, K.; Krayer, M.; Kim, H.-J.; Lindsey, J. S. *New J. Chem.* **2011**, *35*, 1376–1384.

(5) "Synthesis and Photochemical Characterization of Stable Indium Bacteriochlorins," Krayer, M.; Yang, E.; Kim, H.-J.; Kee, H. L.; Deans, R. M.; Sluder, C. E.; Diers, J. R.; Kirmaier, C.; Bocian, D. F.; Holten, D.; Lindsey, J. S. *Inorg. Chem.* **2011**, *50*, 4607–4618.

(6) "Photophysical Properties and Electronic Structure of Stable, Tunable Synthetic Bacteriochlorins: Extending the Features of Native Photosynthetic Pigments," Yang, E.; Kirmaier, C.; Krayer, M.; Taniguchi, M.; Kim, H.-J.; Diers, J. R.; Bocian, D. F.; Lindsey, J. S.; Holten, D. *J. Phys. Chem. B* **2011**, *115*, 10801–10816.

(7) "A *trans*-AB-Bacteriochlorin Building Block," Mass, O.; Lindsey, J. S. *J. Org. Chem.* **2011**, *76*, 9478–9487.

(8) "Effects of Substituents on Synthetic Analogs of Chlorophylls. Part 3: The Distinctive Impact of Auxochromes at the 7- *versus* 3-Positions," Springer, J. W.; Faries, K. M.; Kee, H. L.; Diers, J. R.; Muthiah, C.; Mass, O.; Kirmaier, C.; Lindsey, J. S.; Bocian, D. F.; Holten, D. *Photochem. Photobiol.* **2012**, *88*, 651–674.

(9) "Synthesis and Physicochemical Properties of Metallobacteriochlorins," Chen, C.-Y.; Sun, E.; Fan, D.; Taniguchi, M.; McDowell, B. E.; Yang, E.; Diers, J. R.; Bocian, D. F.; Holten, D.; Lindsey, J. S. *Inorg. Chem.* **2012**, *51*, 9443–9464.

(10) "Stable Synthetic Bacteriochlorins for Photodynamic Therapy: Role of Dicyano Peripheral Groups, Central Metal Substitution (2H, Zn, Pd), and Cremophor EL Delivery," Huang, Y.-Y.; Balasubramanian, T.; Yang, E.; Diers, J. R.; Bocian, D. F.; Lindsey, J. S.; Holten, D.; Hamblin, M. R. *ChemMedChem* **2012**, *7*, 2155–2167. *The studies utilized compounds characterized during the course of the fundamental solar-energy research sponsored by DOE. Attributions to DOE by Bocian and Holten only.*

(11) "Effects of Linker Torsional Constraints on the Rate of Ground-State Hole Transfer in Porphyrin Dyads," Hondros, C. J.; Aravindu, K.; Diers, J. R.; Holten, D.; Lindsey, J. S.; Bocian, D. F. *Inorg. Chem.* **2012**, *51*, 11076–11086.

(12) "Synthesis and Characterization of Lipophilic, Near-Infrared Absorbing Metallobacteriochlorins," Sun, E.; Chen, C.-Y.; Lindsey, J. S. *Chem. J. Chin. Univ.* **2013**, *34*, 776–781.

(13) "Molecular Electronic Tuning of Photosensitizers to Enhance Photodynamic Therapy: Synthetic Dicyanobacteriochlorins as a Case Study," Yang, E.; Diers, J. R.; Huang, Y.-Y.; Hamblin, M. R.; Lindsey, J. S.; Bocian, D. F.; Holten, D. *Photochem. Photobiol.* **2013**, *89*, 605–618. *The studies utilized compounds characterized during the course of the fundamental solar-energy research sponsored by DOE. Attributions to DOE by Bocian and Holten only.*

(14) “Photophysical Properties and Electronic Structure of Bacteriochlorin–Chalcones with Extended Near-Infrared Absorption,” Yang, E.; Ruzié, C.; Krayer, M.; Diers, J. R.; Niedzwiedzki, D. M.; Lindsey, J. S.; Bocian, D. F.; Holten, D. *Photochem. Photobiol.* **2013**, *89*, 586–604.

(15) “Distinct Photophysical and Electronic Characteristics of Strongly Coupled Dyads Containing a Perylene Accessory Pigment and a Porphyrin, Chlorin, or Bacteriochlorin,” Wang, J.; Yang, E.; Diers, J. R.; Niedzwiedzki, D. M.; Kirmaier, C.; Bocian, D. F.; Lindsey, J. S.; Holten, D. *J. Phys. Chem. B* **2013**, *117*, 9288–9304.

(16) “Serendipitous Synthetic Entrée to Tetradehydro Analogues of Cobalamins,” Deans, R. M.; Mass, O.; Diers, J. R.; Bocian, D. F.; Lindsey, J. S. *New J. Chem.* **2013**, *37*, 3964-3975.

(17) “Synthesis and Photophysical Properties of Chlorins Bearing 0–4 Distinct Meso-Substituents,” Aravindu, K.; Kim, H.-J.; Taniguchi, M.; Dilbeck, P. L.; Diers, J. R.; Bocian, D. F.; Holten, D.; Lindsey, J. S. *Photochem. Photobiol. Sci.* **2013**, *12*, 2089-2109.

(18) “Photophysical Properties and Electronic Structure of Retinyledene-Chlorin-Chalcones and Analogues,” Springer, J. W.; Taniguchi, M.; Krayer, M.; Ruzié, C.; Diers, J. R.; Niedzwiedzki, D. M.; Bocian, D. F.; Lindsey, J. A.; Holten, D. *Photochem. Photobiol. Sci.* **2014**, *13*, 634-650.

(19) “Probing Electronic Communication for Efficient Light-Harvesting Functionality: Dyads Containing a Common Perylene and a Porphyrin, Chlorin, or Bacteriochlorin,” Yang, E. K.; Wang, J.; Diers, J. R.; Niedzwiedzki, D. M.; Kirmaier, C.; Bocian, D. F.; Lindsey, J. S.; Holten, D. *J. Phys. Chem. B.* **2014**, *118*, 1630-1647.

(20) “Synthesis of 24 Bacteriochlorin Isotopologues, Each Containing a Symmetrical Pair of 13C or 15N Atoms in the Inner Core of the Macrocycle,” Chih-Yuan Chen, David F. Bocian, and Jonathan S. Lindsey, *J. Org. Chem.* **2014**, *79*, 1001-1016.